A New Algorithm for Border Description of Polarized Light Surface Microscopic Images of Pigmented Skin Lesions

Costantino GRANA, Giovanni PELLACANI, Rita CUCCHIARA, and Stefania SEIDENARI

***Abstract* — The aim of this study was to provide mathematical descriptors for the border of pigmented skin lesion images and to assess their efficacy for distinction among different lesion groups. New descriptors such as Lesion slope (LS) and Lesion Slope Regularity (LSR) are introduced and mathematically defined. A new algorithm based on the Catmull-Rom spline method and the computation of the gray level gradient of points extracted by interpolation of normal direction on spline points was employed. The efficacy of these new descriptors was tested on a data set of 510 pigmented skin lesions, composed by 85 melanomas and 425 nevi, by employing statistical methods for discrimination between the 2 populations.**

***Index Terms* — border, Catmull-Rom splines, skin tumor, melanoma, epiluminescence, image analysis**

I. INTRODUCTION

AID for melanoma diagnosis can be provided by skin surface microscopy which enables the observation of subsurface structures of pigmented skin lesions [1], [2]. However, the increase in diagnostic accuracy, obtained by this method, when based on subjective pattern analysis, has a strong dependency on the dermatologists' experience [3], [4]. Moreover, in spite of a reference terminology [5], [6], some descriptors are probably insufficiently defined, leading to a great inter- and intra-observer variability [7]. In order to increase the reproducibility of clinical judgement, some semiquantitative algorithms have been developed [8], [9] based either on the evaluation of shape and pigment distribution, asymmetry, regularity of the border, colors and differential structures inside the lesion (ABCD rule of dermatoscopy) [8] or on pattern analysis (new 7 point checklist) [9].

The description of the border aspect appears to be an important feature for clinical judgement [1], [2], [8], [10]-[12]. Some border descriptors, such as border irregularity and the presence of abrupt border cut-off, have been considered as predictors of malignancy. However, the interpretation of these parameters is still subjective and can lead to different results depending on the examiner.

Programs for image analysis enable the numerical description of some aspects of pigmented skin lesions [13-20], providing a reproducible quantification of several features and an aid for clinical diagnosis. Different approaches for an objective and quantitative description of the border of the lesion have been developed. Parameters such as the "lesion gradient" [15], the "skin lesion gradient" [16], [18]-[20], and the "maximum and minimum border width" [17] were introduced, but insufficiently defined. Moreover, the luminance values along a radial direction from the center of the lesion to the surrounding skin [14] and the difference between the average color values in the peripheral regions inside and outside the contour line [13] were calculated and implemented as border descriptors. Recently, an interesting algorithmic reproduction of the "B" parameter of the ABCD rule of dermatoscopy, which automatically measures the number of segments with sharp cut-off, was described [21].

We propose a new mathematical approach to the assessment of the lesion boundary, which considers luminance values along a direction normal to the contour at each point. This method enables the precise evaluation of the contours also of lesions with deep indentations and irregular shape. Numerical description of different border features was obtained. Subsequently, we tested the border parameters on a set of melanoma and melanocytic nevus images in order to evaluate the capability of these descriptors in distinguishing between the two groups.

II. MATERIALS AND METHODS

A. Study population and instrument

A total of 510 images of pigmented skin lesions, referring to 85 melanomas and 425 melanocytic nevi. The lesions included in this study were all considered equivocal from a clinical point of view and had been excised for histopathologic examination. Prior to biopsy, images were acquired by means of a digital

Manuscript received May 6, 2002; revised August 27 and November 14, 2002.

S. Seidenari and G. Pellacani, Department of Dermatology, University of Modena and Reggio Emilia, 41100 Modena, Italy (e-mail: seidenari.stefania@unimo.it; pellacani.giovanni@unimo.it).

C. Grana and R. Cucchiara, Department of Computer Engineering, University of Modena and Reggio Emilia, 41100 Modena, Italy (e-mail: grana.costantino@unimo.it; cucchiara.rita@unimo.it).

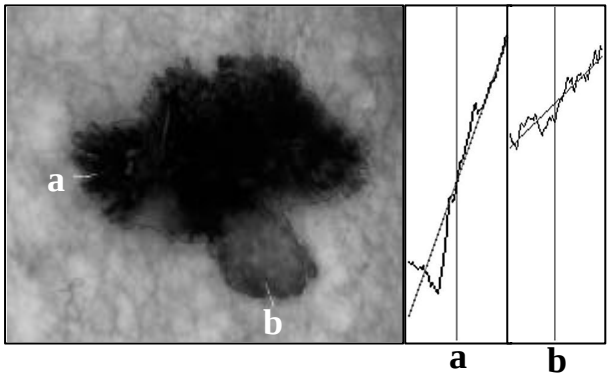

Fig. 1. Example of the resulting slope values obtained by the least squares method. Two different situations are highlighted within the same lesion (melanoma, thickness 0.29 mm). In the first detail (a) a sharp cut-off is shown, while in the second one (b) a fuzzy border is found.

videomicroscope (NTSC VMS-110A, Scalar Mitsubishi, Tamashi, Tokyo, Japan), with a 20 fold magnification enabling the whole lesion to be included in the monitor area. The instrument has been described elsewhere [16]. The images were digitized by means of a Matrox Orion frameboard and stored by an image acquisition program (VideoCap 8.09, DS-Medica, Milan, Italy), which runs under Microsoft Windows. The digitized images offer a spatial resolution of 640 x 480 pixels and a color resolution of 16 million colors.

B. Border analysis

The aim of this section is to give a clear definition of the lesion slope and its operative description. We define *Lesion Slope* (LS) the numerical measure that describes the swiftness at which the lesion merges into the skin. To build this global measure we need first of all to obtain the border of the lesion, then a local direction along which we can measure the gradient and finally a formal measure for the gradient along the slope direction.

Given an image space $I = \{\mathbf{p} = (x, y) : 0 < x < w \wedge 0 < y < h\}$ our image is regarded as a function $f : I \to RGB_0^{255}$ where *R,G,B* are the nonlinear red, green and blue color components. After acquisition, the color image is converted into a luminance image $g : I \to Y_0^{255}$ defined according to ITU-R Recommendation BT. 601 (formerly CCIR Rec. 601) as follows:

$$Y = 0.299R + 0.587G + 0.114B \tag{1}$$

The first step consists in the lesion border detection, i.e. finding the set $B = (b_i \in I, i = 1 \ldots N)$. The boundary of the lesion is obtained by simple segmentation, applying a threshold to the luminance image. The threshold value able to distinguish between skin and lesion is automatically computed for each image using the algorithm developed by Otsu [22]. This algorithm first computes the histogram of the gray level image and then determines the binarization threshold. The threshold selection is based on the maximization of the interclass variance assuming that the image is composed by only two classes. The binarized image is then labeled and the largest connected component is kept as the lesion. A one pixel wide line, following the smallest indentation of the contour, is obtained by means of a chain-code procedure.

The contour obtained by this method is then evaluated by an experienced dermatologist. When clinical evaluation does not correspond to the automatic segmentation, the threshold is interactively modified over selected windows of the image space *I*. In our cases, a correct border detection was automatically obtained in 191 out of 210 images (90.4%). In the remaining 19 cases where the border was not exactly defined, due to only slight differences between lesion color and colors in the surrounding skin area, the border was manually corrected. The automatic border segmentation rate was comparable to previous results, where the percentage of completely automatic border detection ranged from 60 to 96% [23]-[25].

In order to obtain a smoother outline, an interpolation approach based on spline curves is used. The spline curve is constructed selecting one pixel every *k* as control points. The *k* pixel step is set heuristically to 10, because it allows small indentations to be rejected without losing important details, at the magnification level used. Spline curves are built by the composition of a set of piecewise polynomial third order functions. For our purposes the Catmull-Rom splines, characterized by the quality that the resulting curve crosses all the interpolated points, were chosen [26].

Catmull-Rom splines are defined on a continuos interval $t \in [0,1]$, between each pair of control points $\mathbf{p}_i, \mathbf{p}_{i+1}$, by the following parametric equation:

$$\mathbf{q}_i(t) = \frac{1}{2}\begin{bmatrix} t^3 & t^2 & t & 1 \end{bmatrix}\begin{bmatrix} -1 & 3 & -3 & 1 \\ 2 & -5 & 4 & -1 \\ -1 & 0 & 1 & 0 \\ 0 & 2 & 0 & 0 \end{bmatrix}\begin{bmatrix} \mathbf{p}_{i-1} \\ \mathbf{p}_i \\ \mathbf{p}_{i+1} \\ \mathbf{p}_{i+2} \end{bmatrix} \tag{2}$$

This equation defines a continuos function from point $\mathbf{p}_i$ to point $\mathbf{p}_{i+1}$, whose tangents in $\mathbf{p}_i$ and $\mathbf{p}_{i+1}$ are equal to $\frac{\mathbf{p}_{i+1} - \mathbf{p}_{i-1}}{2}$ and $\frac{\mathbf{p}_{i+2} - \mathbf{p}_i}{2}$. The resulting contour is drawn varying *i* from 0, the starting point, to *N*, the last control point, moving clockwise on the border. *k* boundary points per piece of spline curve between two consecutive control points are considered.

The mathematical representation of the border enabled us to define the *Slope Direction* as the direction normal to the spline at each point. This is computed taking the first derivative of the parametric equation:

$$\frac{d\mathbf{q}_i(t)}{dt} = \frac{1}{2}\begin{bmatrix} t^2 & t & 1 & 0 \end{bmatrix}\begin{bmatrix} -3 & 9 & -9 & 3 \\ 4 & -10 & 8 & -2 \\ -1 & 0 & 1 & 0 \\ 0 & 0 & 0 & 0 \end{bmatrix}\begin{bmatrix} \mathbf{p}_{i-1} \\ \mathbf{p}_i \\ \mathbf{p}_{i+1} \\ \mathbf{p}_{i+2} \end{bmatrix} \quad (3)$$

and then building the normal versor as

$$\hat{\mathbf{q}}_i(t) = \frac{1}{\left\| \frac{d\mathbf{q}_i(t)}{dt} \right\|}\begin{bmatrix} \frac{dy_i(t)}{dt} \\ -\frac{dx_i(t)}{dt} \end{bmatrix}. \quad (4)$$

To measure the skin lesion gradient, defined as the change in lightness from the lesion to the skin, at each boundary point, l lightness values, half inside and half outside the border, are extracted on an l pixel long segment, centered on the boundary point and oriented according to the Slope Direction. The points are thus defined according to the following equation:

$$\mathbf{d}_j(\mathbf{q}_i, t) = \mathbf{q}_i(t) + \left(j - \tfrac{l}{2}\right)\hat{\mathbf{q}}_i(t),\ j = 1,\ldots,l \quad (5)$$

and extracted using bilinear interpolation.

The l lightness values can be graphed by position from the inside to the outside of the lesion (Fig. 1). The gradient at each border point was formally defined as the slope of the data, calculated by the method of the least squares. Under suitable hypothesis we search the parameters for the best fitting line $h(j; m, q) = mj + q$, in order to minimize the error measure:

$$e^2 = \sum_{j=1}^{l}\left(g(\mathbf{d}_j) - mj - q\right)^2 \quad (6)$$

By taking the partial derivatives with respect to m and q, we obtain the measure for the gradient as

$$m = \frac{l\sum_{j=1}^{l} j g(\mathbf{d}_j) - \sum_{j=1}^{l} j \sum_{j=1}^{l} g(\mathbf{d}_j)}{l\sum_{j=1}^{l} j^2 - \left(\sum_{j=1}^{l} j\right)^2}. \quad (7)$$

Two conditions are tested to insure a correct evaluation: 1) the segment has to be completely included in the image boundaries and 2) it must cross the border only once.

In order to numerically describe the gradient at the border for each lesion, we defined the mean of the slope values at each boundary point as *Lesion Slope (LS)* and its standard deviation as *Lesion Slope Regularity (LSR)*.

Subsequently, the lesion was divided automatically into 8 segments using 4 axes separated from each other by a 45° angle, starting from the major axis in order to avoid the rotation influence on segment characterization. The mean and the standard deviation of the slope values were calculated for each segment (sS_i = segment slope and sSR_i = segment slope regularity). For each lesion only the highest and lowest segment slope and segment slope regularity values were considered (sS_{min}, sS_{max}, sSR_{min}, sSR_{max}).

C. Statistics

In order to verify and to validate our method for border description, the study population was consecutively divided into a training set comprising 210 lesions (60 melanomas and 150 melanocytic nevi) and a test set comprising 300 lesions (25 melanomas and 275 melanocytic nevi).

TABLE I
MEAN AND STANDARD DEVIATION OF THE BORDER PARAMETERS OBTAINED ON THE IMAGES OF 425 NEVI AND 85 MELANOMAS

		Training set		Test set	
Border Parameters		Nevi (150)	Melanomas (60)	Nevi (275)	Melanomas (25)
LS	Lesion Slope	2.389 ± 0.609	3.182 ± 0.930*	2.616 ± 0.758	3.121 ± 1.056*
LSR	Lesion Slope Regularity	0.681 ± 0.119	0.958 ± 0.316*	0.676 ± 0.141	0.935 ± 0.260*
SS_{min}	Minimum Segment Slope	2.137 ± 0.592	2.900 ± 0.905*	2.036 ± 0.752	2.293 ± 1.142
SS_{max}	Maximum Segment Slope	2.636 ± 0.647	3.473 ± 0.931*	3.236 ± 0.813	4.238 ± 0.980*
SSR_{min}	Minimum Segment Slope Regularity	0.485 ± 0.111	0.747 ± 0.285*	0.344 ± 0.084	0.390 ± 0.112*
SSR_{max}	Maximum Segment Slope Regularity	0.821 ± 0.153	1.116 ± 0.342*	0.760 ± 0.180	1-007 ± 0.244*

* significant in respect to nevi

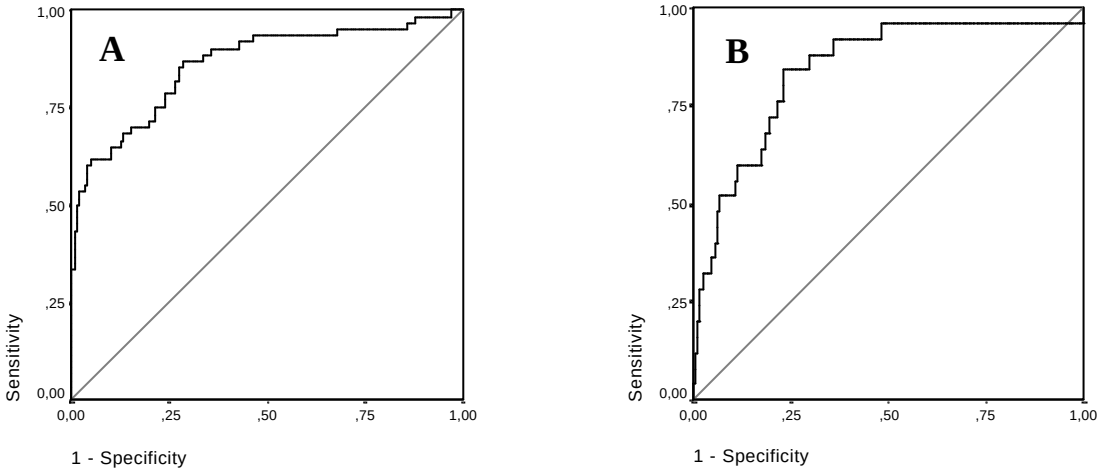

Fig. 2. ROC curves for D score in the detection of melanomas. A) Training set (AUC = 0.861); B) Test set (AUC = 0.842)

As basic statistics mean and standard deviation of LS, LSR, sS_{min}, sS_{max}, sSR_{min}, sSR_{max} were calculated for melanomas and nevi both in the training and in the test set. Significant differences between nevus and melanoma values were evaluated using the Mann-Whitney U test for independent samples. A p value <0.05 was considered significant.

The values referring to parameters belonging to the training set underwent elaboration by means of multivariate discriminant analysis, as implemented in the SPSS statistical package (release 10.0.06, 1999; SPSS Inc., Chicago, Ill.). Discriminant analysis enables the identification of variables, which are important for distinction among the groups (training set) and develops a procedure for predicting group membership for new cases in which group membership is undetermined (test set). A linear combination of independent variables is formed and serves as a basis for assigning cases to groups. A score (D) is obtained for each lesion by the linear discriminant equation $D=B_0+B_1X_1+B_2X_2...+B_nX_n$, where the X_s are the values of the independent variables and the B_s are coefficients estimated from the data of the training set. Going on the training set data, a threshold score is automatically established for the attribution of cases to groups. The same value was employed for discriminating benign and malignant lesions belonging to the test set.

Receiver operating characteristic (ROC) analysis [27] was performed on the training and test set values in order to investigate sensitivity and specificity of the discriminant equation on pigmented skin lesion classification. The ROC analysis provides a means to assess the overall discriminant power. For each cut-off, an instrument has a sensitivity (true positive rate) and a specificity (true negative rate). High values of these coefficients are desirable, although they are inversely related. ROC curves can be obtained by plotting the false-positive rate and the true positive rate for different thresholds of the discriminant score D. Diagnostic accuracy was estimated by the ratio between the percentage of the sum of true positives and true negatives, and the total number of lesions and it was calculated for each threshold (D) value. The area under the curve (AUC) is the most commonly used index to assess the overall discriminant power of an instrument. To calculate this area, the nonparametric trapezoidal method was employed. The AUC varies between 0.50, which corresponds to the chance line, and 1.0, a value associated with perfect accuracy. This parameter can be interpreted as the probability of correctly classifying the subjects of a pair in which one is normal and one is diseased.

For the estimate of the melanoma risk, the calculation of the odds ratio (OR) and 95% confidence interval (C.I.95%) was performed considering the D score value with the best diagnostic accuracy as the threshold value.

III. Results

Mean and standard deviation of each parameter calculated for training and test set are listed in Table I. Melanomas had significantly higher values in comparison with nevi for all the parameters except SS_{min} for the training set.

Employing the discriminant analysis approach, all the parameters appeared useful for distinction between nevi and melanomas. The equation developed on the training set for the classification into two groups was:

$D = (1.399*LS) + (5.102*LSR) + (1.438*sS_{min}) + (1.354*sS_{max}) + (5.600*sSR_{min}) + (4.471*sSR_{max}) + (-21.9)$

Mean and Standard deviation of D values were -2.051 ± 3.533 for nevi and 5.485 ± 6.145 for melanomas belonging to the training set and -2.160 ± 3.468 for nevi and 2.961 ± 4.654 for melanomas belonging to the test set.

Fig. 2 shows the ROC curves for D scores for distinction between melanomas and nevi belonging to the training and test set respectively. The AUC value was 0.861 for the training set and 0.842 for the test set. Table II shows the sensitivity,

specificity and diagnostic accuracy values obtained for each D score cut-off point on the overall population. For a D score equal to 0, a 85.9% sensitivity and a 74.1% specificity, with a diagnostic accuracy of 80.0%, were obtained. According to odds ratio calculation, a D score greater than 0 was highly predictive for melanoma (OR=17.42; C.I.95% 9.11-33.30).

TABLE II
SENSITIVITY, SPECIFICITY AND DIAGNOSTIC ACCURACY VALUES AT VARIOUS CUT-OFF POINTS OF D SCORE FOR DETECTION OF MELANOMAS

D score cut-off point	Sensitivity (%)	Specificity (%)	Diagnostic accuracy (%)
-12.46	100.00	0.00	50.00
-7.94	97.65	5.41	51.53
-5.88	96.47	14.35	55.41
-4.98	95.29	19.06	57.18
-3.98	95.29	28.47	61.88
-3.30	94.12	38.35	66.24
-2.81	94.12	43.76	68.94
-2.03	94.12	51.76	72.94
-1.62	91.76	55.53	73.65
-1.09	90.59	63.53	77.06
-0.68	87.06	67.76	77.41
-0.26	85.88	71.29	78.59
0	**85.88**	**74.12**	**80.00**
0.26	77.65	76.24	76.94
0.62	72.94	79.06	76.00
1.55	67.06	86.59	76.82
2.11	63.53	90.12	76.82
3.08	56.47	92.47	74.47
4.14	50.59	95.76	73.18
5.28	44.71	97.18	70.94
6.08	42.35	98.35	70.35
7.39	28.24	99.53	63.88
9.18	18.82	99.76	59.29
11.81	14.12	100.00	57.06
19.78	0.00	100.00	50.00

Numbers in boldface indicate best diagnostic accuracy

IV. DISCUSSION

In dermatoscopy, the diagnosis is based both on the evaluation of some general features of the lesion, such as color, shape and border, and on the presence and the aspect of characteristic structures, such as pigment network, globules and others [1], [2], [8]-[12]. Perception of these structures depends both on magnification and image resolution. The informativeness of our digital images was previously successfully checked in studies concerning the identification of melanomas, melanocytic nevi and Spitz nevi [16], [28]. Lesion features are helpful for experienced investigators, but their evaluation is sometimes not fully reproducible [3], [4], [7], [29]. Both the global pattern analysis and the ABCD rule for dermatoscopy consider the border as a relevant parameter. The first method evaluates the "regularity" of the margin, defining the border "regular" when a thinning out of the pigmentation into the surrounding skin is observable and "irregular" for the presence of abrupt stops of the pigment at the edge [1], [2], [11], [12]. With the ABCD rule, the "B" score, ranging from 1 to 8, is attributed on the basis of the number of segments with an abrupt edge interruption of the pigment. A value ranging from 0 to 0.8 (deriving from the multiplication of border score by a coefficient) is then added to the scores for symmetry, color and differential structures, contributing to less then 10% of the final score [8]. A consensus net meeting based on the evaluation of 128 pigmented skin lesion images by 40 observers identified the presence of abrupt border cutoffs in not less and not more than 3-5 out of 8 border segments as associated with melanoma (OR=2.6), indicating that the non homogeneity of the border (corresponding to high LSR values) is the main parameter characterizing the border of malignant lesions [29]. Moreover, both clinical and semiquantitative methods are not error proof, since the clinical judgement on a single feature is based on the visual impression, which is not able to exclude the general aspect of the lesion. The visual cortex tries to sharpen the edge, especially when a lesion is heavily pigmented, leading to non reproducible and sometimes incorrect evaluations.

The introduction of digital-epiluminescence microscopy, associated with image processing techniques, enables the numerical and objective description of some pigmented skin lesion features. In most programs for image analysis of pigmented skin lesions, the transition between lesion and skin is assessed and quantified, using different approaches, which have not been clearly defined in most cases. The parameters "skin-lesion gradient" and "lesion gradient", respectively given by the Burroni-Dell'Eva method [16], [18]-[20] and by Gutkowicz-Krusin et al. [15], describe the difference in color between healthy skin and the lesion, but no mathematical description is available. The terms "area of the border" and "maximum and minimum border width" were introduced by Binder et al. for the border quantification, without any further detail on their meaning [17]. Hall et al. calculated the edge blur unwinding the lesion and taking vertical profiles of the results, and obtained the variation of the gray level from the center of the lesion to the skin along a radial direction [14]. Schindewolf et al. evaluated a 40 pixel wide band constructed around the lesion border: the difference between the average CIE-DIN color values in the two halves was the measure of the transition [13]. Day introduced a method to algorithmically reproduce the border cut-off criterion of the ABCD rule for dermatoscopy by dividing the lesion into 8 segments and calculating the maximum change in lightness from lesion to skin in 5 equidistant points per each segment: 8 real numbers, representing the border cut-off, were obtained [21]. The detection of the border is important in computer-assisted diagnosis of melanoma, also because, depending on the performance of this step, assessment of symmetry of the lesion will vary, influencing the classification into malignant or benign.

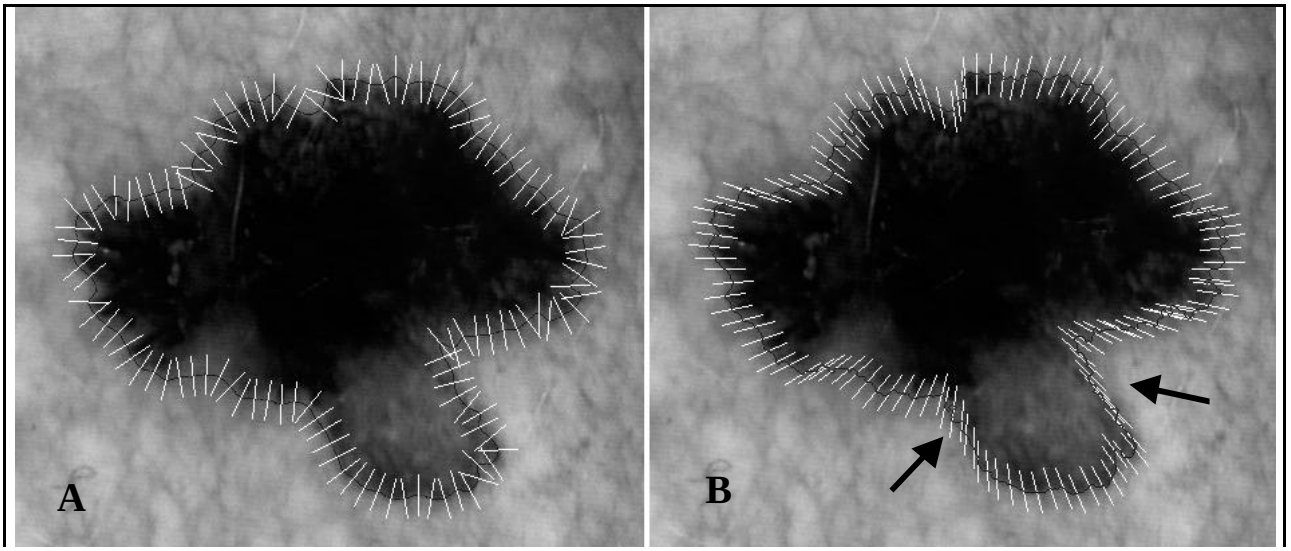

Fig. 3. Melanoma image with a representation of sample segments along which the border gradient is calculated, following (A) normal direction (as implemented by the proposed new algorithm) and (B) radial direction (as usually implemented by other systems [14] -[21]). The example shows that in lesions with irregular shape the use of the radial direction gives rise to incorrect evaluations of border gradient for wide tracts of the lesion (as represented in the portions indicated by the black arrows).

We developed a completely automatic system for border description which produces different numerical parameters related to different border features. The border correction by means of the Catmull-Rom splines was chosen in order to obtain a smoother outline, without losing important details on the real shape of the border. In our method, to measure the skin-lesion gradient, a segment oriented along the normal direction, instead of one oriented according to the radial direction [14]-[21], was chosen, enabling the precise evaluation of the change in lightness from the lesion to the skin also in border tracts with deep indentations (Fig. 3). The LS values described the overall intensity of the skin-lesion gradient at the border, whereas LSR was an indicator of the "unhomogeneity" of the border cut-off. In our study, the increased LS and LSR showed that melanomas have more abrupt and unhomogeneous margins. The same parameters were calculated in each of the 8 segments in to which the lesion was divided, and the highest and lowest values obtained for each lesion were reported (sS_{min}, sS_{max}, sSR_{min}, sSR_{max}). All these parameters were higher in melanomas. In particular, the higher values of sS_{max} and sSR_{max} can be explained by the presence of peripheral structures, such as pseudopods or radial streaming, constituted by heavily pigmented extensions of the margin into the surrounding skin. Applying discriminant analysis on test set data, all border descriptors appeared useful in distinguishing between nevi and melanomas. Testing the equation in blind on a new pigmented skin lesion population, previous results were confirmed demonstrating the clinical efficacy of the algorithm.

In conclusion, by this method, the border parameters are automatically obtained and numerically described, avoiding errors due to human perception. Obviously, the border parameters alone are not able to correctly classify all melanomas by discriminant analysis, similarly to clinical diagnosis which is not only based on the observation of the lesion border. However, this automatic method provides numerical values corresponding to an odds ratio which is much more predictive for melanoma than the one obtained by the clinical evaluation of the border cut-off ("automatic" OR =17.4 versus "clinical" OR=2.6 [29]).

This method represents a contribution to the refinement of programs for image analysis, based on the description of different lesion features, implemented with an automatic classifier. Computer diagnosis available for experts and for less experienced dermatologists always supported by clinical examination, may allow a wider diffusion of surface microscopic techniques and, consequently, an increase in diagnostic accuracy especially for thin melanomas. In an effort to encourage reproduction and improvement of this research, and to compare our algorithm for border description with others under research, both the algorithm and image set employed are available for use. For details, contact the corresponding author (seidenari.stefania@unimo.it).

REFERENCES

[1] H. Pehamberger, A. Steiner, and K. Wolff, "In vivo epiluminescence microscopy of pigmented skin lesions. I. Pattern analysis of pigmented skin lesions," *J. Am. Acad. Dermatol.*, vol. 17, pp. 571-583, 1987.

[2] R. O. Kenet, S. Kang, B. J. Kenet, T. B. Fitzpatrick, A. J. Sober, and R. L. Barnhill, "Clinical diagnosis of pigmented lesions using digital epiluminescence microscopy," *Arch. Dermatol.*, vol. 129, pp. 157-174, 1993.

[3] M. Binder, M. Schwarz, A. Winkler, et al., "Epiluminescence microscopy. A useful tool for the diagnosis of pigmented skin lesions for formally trained dermatologists," *Arch. Dermatol.*, vol. 131, pp. 286-291, 1995.

[4] I. Stanganelli, S. Seidenari, M. Serafini, G. Pellacani, and L. Bucchi, "Diagnosis of pigmented skin lesions by epiluminescence microscopy: determinants of accuracy improvement in a nationwide training programme for practical dermatologists," *Public Health*, 113, pp. 237-242, 1999.

[5] F.A. Bahmer, P. Fritsch, J. Kreusch, H. Pehamberger, C. Rohrer, I. Schindera, J. Smolle, H. P. Soyer, and W. Stolz, "Terminology in surface microscopy," *J. Am. Acad. Dermatol.*, 23, pp. 1159-1162, 1990.

[6] H. P. Soyer, G. Argenziano, S. Chimenti, S. W. Menzies, H. Pehamberger, H. S. Rabinovitz, W. Stolz, and A. W. Kopf, eds. Dermoscopy of Pigmented skin lesions. An atlas based on the consensus net meeting on dermoscopy 2000. Milan, Italy: EDRA; 2001.

[7] I. Stanganelli, M. Burroni, S. Rafanelli, and L. Bucchi, "Intraobserver agreement in interpretation of digital epiluminescence microscopy," *J. Am. Acad. Dermatol.*, 33, pp. 584-589, 1995.

[8] F. Nachbar, W. Stolz, T. Merkle, A. B. Cognetta, T. Vogt, M. Landthaler, P. Bilek, O. Braun-Falco, and G. Plewig, "The ABCD rule of dermatoscopy," *J. Am. Acad. Dermatol.*, 30, pp. 551-559, 1994.

[9] G. Argenziano, G. Fabbrocini, P. Carli, V. De Giorgi, E. Sammarco, and M. Delfino, "Epiluminescence microscopy for the diagnosis of doubtful melanocytic skin lesions. Comparison of the ABCD rule of dermoscopy and a new 7-point checklist based on pattern analysis," *Arch. Dermatol.*, 134, pp. 1563-1570, 1998.

[10] H. Pehamberger, M. Binder, A. Steiner, and K. Wolff, "Early recognition and prognostic markers of melanoma," *Melanoma Res.*, 3, pp. 279-284, 1993.

[11] A. Steiner, M. Binder, M. Schemper, K. Wolff, and H. Pehamberger, "Statistical evaluation of epiluminescence microscopy criteria for melanocytic pigmented skin lesions," *J. Am. Acad. Dermatol.*, 29, pp. 581-588, 1993.

[12] M. Nilles, R. H. Boedeker, and W. B. Schill, "Surface microscopy of naevi and melanomas – clues to melanoma," *Br. J. Dermatol.*, 130, pp. 349-355, 1994.

[13] T. Schindewolf, W. Stolz, R. Albert, W. Abmayr, and H. Harms, "Classification of melanocytic lesions with color and texture analysis using digital image processing," *Analyt. Quant. Cytol. Histol.*, 15, pp. 1-11, 1993.

[14] P. N. Hall, E. Claridge, and J. D. Morris Smith, "Computer screening for early detection of melanoma – is there a future?" *Br. J. Dermatol.*, 132, pp. 325-338, 1995.

[15] D. Gutkowicz-Krusin, M. Elbaum, P. Szwaykowski, and A. W. Kopf, "Can early malignant melanoma be differentiated from atypical melanocytic nevus by in vivo techniques? Part II. Automatic machine vision classification," *Skin Res. Technol.*, 3, pp. 15-22, 1997.

[16] S. Seidenari, G. Pellacani, and P. Pepe, "Digital videomicroscopy improves diagnostic accuracy for melanoma," *J. Am. Acad. Dermatol.*, 39, pp. 175-181, 1998.

[17] M. Binder, H. Kittler, A. Seeber, A. Steiner, H. Pehamberger, and K. Wolff, "Epiluminescence microscopy-based classification of pigmented skin lesions using computerized image analysis and an artificial neural network," *Melanoma Res.*, 8, pp. 261-266, 1998.

[18] S. Seidenari, G. Pellacani, and A. Giannetti, "Digital videomicroscopy and image analysis with automatic classification for detection of thin melanomas," *Melanoma Res.*, 9, pp. 163-171, 1999.

[19] L. Andreassi, R. Perotti, P. Rubegni, M. Burroni, G. Cevenini, M. Biagioli, P. Taddeucci, G. Dell'Eva, and P. Barbini, "Digital dermoscopy analysis for the differentiation of atypical nevi and early melanoma," *Arch. Dermatol.*, 135, pp. 1459-1465, 1999.

[20] G. Pellacani, M. Martini, and S. Seidenari, "Digital videomicroscopy with image analysis and automatic classification as an aid for diagnosis of Spitz nevus," *Skin Res. Technol.*, 5, pp. 266-272, 1999.

[21] D. Day, "How blurry is that border? An investigation into algorithmic reproduction of skin lesion border cut-off," *Computerized Medical Imaging and Graphics*, 24, pp. 69-72, 2000.

[22] N. Otsu, "A Threshold Selection Method for Gray-Level Histograms," *IEEE Transaction on Systems, Man and Cybernetics*, 9, pp. 62-66, 1979.

[23] A. Green, N. Martin, J. Pfitzner, M. O'Rourke, and N. Knight, "Computer image analysis in the diagnosis of melanoma," *J. Am. Acad. Dermatol.*, 31, pp.958-964, 1994.

[24] G.A. Hance, S.E. Umbaugh, R.H. Moss, and W.S. Stoecker, "Unsupervised color image segmentation," *IEEE Eng. Med. Biol. Mag.*, 15, pp. 104-111, 1996.

[25] H. Ganster, A. Pinz, R. Rohrer, E. Wildling, M. Binder, and H. Kittler, "Automated Melanoma Recognition," *IEEE Trans. Med. Imaging*, 20, pp.233-239, 2001.

[26] E. Catmull, and R. Rom, "A Class of Local Interpolationg Splines," in *Computer Aided Geometric Design*, R. E. Barnhill and R. F. Riesened, Eds. New York: Academic Press, 1974.

[27] J. A. Hanley, and B. J. McNeil, "The meaning and use of the area under a receiver operating characteristic (ROC) curve," *Radiology*, 143, pp. 29-36, 1982.

[28] G. Pellacani, A.M. Cesinaro and S. Seidenari, "The morphological features of Spitz nevus as observed by digital videomicroscopy," *Acta Derm Venereol*, 80, pp. 117-121, 2000.

[29] G. Argenziano, H.P. Soyer, S. Chimenti, et al., "Dermoscopy of Pigmented Skin Lesions: Results of a Consensus Meeting Via the Internet," *J Am Acad Dermatol*, 2002, in press.